Growth model for metal films on oxide surfaces: Cu on ZnO(0001)-O

K. H. Ernst, A. Ludviksson, R. Zhang, J. Yoshihara, and C. T. Campbell
Department of Chemistry, BG-10, University of Washington, Seattle, Washington 98195
(Received 24 September 1992; revised manuscript received 6 January 1993)

The structural and electronic properties of Cu films vapor deposited on the oxygen terminated ZnO(0001)-O surface at 130 K have been characterized using x-ray photoemission spectroscopy (XPS), He^+-ion-scattering spectroscopy, low-energy electron diffraction work-function and band-bending measurements, angular-resolved XPS, and CO and H_2O chemisorption. These results show that Cu is cationic at tiny coverages, but becomes nearly neutral at coverages beyond a few percent. The Cu clusters into two-dimensional (2D) metallic islands at these coverages. Further deposition of Cu leads to spreading of these 2D islands without forming thicker layers, until about 50% of the surface is covered. Thereafter, these Cu islands grow thicker without filling the gaps between the islands except at a rate much slower than the rate at which Cu is deposited into these clean spaces. The annealing behavior of these films has also been studied between 130 and 850 K. These results show that the Cu has a tendency to cluster into thick 3D islands which only cover a small fraction of the surface. We present a model here based on the energetics of the system which readily explains the apparent contradiction between this tendency for 3D clustering, and the dynamical effect which leads to efficient wetting for coverages up to $\frac{1}{2}$ monolayer at low temperatures. This model shows that a large fraction of the surface can first be covered by a 2D film even when the metal's self-adsorption energy significantly exceeds its adsorption energy on the oxide, provided the difference in these energies does not exceed the energy of 2D evaporation from kinks onto terraces. This model helps to explain a variety of confusing results in the growth of metal films on oxide surfaces.

I. INTRODUCTION

While numerous studies have appeared concerning the growth of metal films on single-crystal metal substrates and their chemisorption properties, relatively few of these types of studies have appeared where single-crystal metal oxides have been used as the substrate. The state of knowledge in that area is still rather rudimentary, with little understanding even of the reasons why some systems show Volmer-Weber growth behavior [three-dimensional (3D) clustering], while others appear to show either layer-by-layer or Stranski-Krastonov behavior at low temperatures, but Volmer-Weber behavior at high temperatures.[1-3] (Here we relax the definitions of these growth modes to include nonequilibrium structures, after Ref. 1.) These systems are nevertheless quite interesting from the point of view of oxide-supported metal catalysts and metal-ceramic interfaces in materials and electronics applications. The Cu/ZnO system is particularly interesting because of its use as a catalyst for methanol synthesis and water-gas shift (Ref. 2 and references therein). The vapor deposition of Cu onto the oxygen-terminated ZnO(0001)-O surface has been studied previously by Campbell, Daube, and White in 1987,[2] and by Didziulis *et al.* in 1989.[3] In both of these studies, the substrate ZnO was maintained at room temperature during Cu deposition. In the present study, we use substrate temperatures down to 120 K, which reveal some interesting new features of the growth mode, requiring reinterpretation of the higher-temperature data. These results lead us to suggest a type of kinetically controlled growth mechanism which has not been previously suggested, but which we propose will be quite common in metal-on-oxide systems.

II. EXPERIMENT

The experiments were performed in an ultrahigh vacuum apparatus with a base pressure of 10^{-10} torr. It had capabilities for x-ray photoelectron spectroscopy (XPS), ion-scattering spectroscopy (ISS), low-energy electron diffraction (LEED), and temperature-programmed desorption (TPD) spectroscopy using a quadrupole mass spectrometer interfaced to a computer for multiplexing masses. The acceptance cone of the Perkin-Elmer Model 10-360 hemispherical analyzer with position-sensitive detector, used for XPS and ISS, was about 3°, so angular resolution was such that the sample could be rotated on one axis. Work-function changes were measured using the onset of the secondary electron distribution in XPS, with a very low-pass energy (5 eV) for high resolution and a negatively biased sample (10.000 V). This method gives the same area-averaged work-function changes that are seen with the Kelvin-probe method, even when patches of adsorbate exist.[4] All XPS spectra reported here used Al $K\alpha$ radiation (1486.6 eV). All ISS spectra were collected using 700-eV He^+ ions at a scattering angle of 135° and a pass energy of 179 eV, which gives an instrumental resolution much better than the inherent peak widths ($\sim$20 eV) due to the physics of the scattering. The detection angle was normal to the surface unless otherwise stated, and the ion beam was incident at a polar angle of 45° from normal, along the $\langle \bar{1}100 \rangle$ azimuth. Its current was about 20 nA, and it took $\sim$30 s to acquire a full spectrum.

 ©1993 The American Physical Society

The two $7\times10\times1.5$-mm^3 ZnO samples used in this study were oriented as purchased (from Atomergic) to $\frac{1}{2}°$ of the 0001 faces. They were etched to determine which face was the oxygen-terminated face (see Ref. 5), and mechanically polished down to 0.06-μm alumina powder. They were briefly sputter cleaned with 700-eV Ar^+ ions, and annealed for some hours at 850 K to obtain a clean surface by XPS and a good (1×1) LEED pattern. Routine cleaning was accomplished with sputtering, followed by 15-min anneals at 850 K. Sometimes the annealing was performed in a doser flux equivalent to 10^{-6} torr of O_2, if it appeared that the O:Zn signal ratio in ISS had decreased below its expected value for the clean, stoichiometric ZnO surface $(1{:}4\pm1)$. In these cases, the O_2 valve was closed before cooling the sample, to ensure that any nonlattice oxygen was desorbed, although cooling in O_2 did not significantly change the signals. When the O:Zn ratio was low, it was because the Zn signal was high. This could be explained by a few percent of oxygen vacancies in the topmost layer. In our previous study of this system,[2] the pass energy in ISS was proportional to the kinetic energy, which naturally leads to a much higher O:Zn ratio than quoted above.

The chemisorption behavior of our thick Cu films grown at 130 K much more closely resembles Cu(110) than Cu(111).[6,7] Assuming therefore that our thick Cu films grown at 130 K (see Fig. 5 below) have a work function like that of Cu(110) (4.48 eV (Ref. 8)), our clean ZnO surface had a work function of 5.18 eV. This value is close to the previously reported value for vacuum-cleaved ZnO(0001)-O of 4.95 eV.[9] The later value was found to be independent of vacuum annealing up to 800 K, as was the (upward) band bending of -0.22 eV,[9] suggesting that our annealing procedure should not cause electronic changes from the perfect surface. This was also confirmed by the observation that the adsorption behavior of our surface toward CO,[6] and its desorption spectrum for H_2O,[7] were unaffected by annealing in oxygen, or using annealing temperatures just below 800 K instead of the usual 850 K after sputtering. The Cu growth behavior, and the CO adsorption behavior on these Cu films reported elsewhere,[6] were independent of the crystal used.

The crystals were mounted on a sample holder for heating, cooling to 100 K, and movement. In both cases, the back of the crystal was polished flat to 1-μm powder, as was the matching surface of a $6\times9\times1.5$-mm^3 Ta plate. The ZnO crystal was attached to this plate using four 0.25-mm Ta wires, which were spot welded to the back of the Ta plate and bent over the front of the plate such that they spring loaded the ZnO to the plate. This plate was mounted to large Ta electrodes on the sample holder using short lengths of 0.25-mm-diameter Ta wire, spot welded to the back of the Ta plate. By placing a voltage across the electrodes, the plate was thus heated. Its temperature was monitored using a thermocouple mounted to its back. Good thermal contact to the ZnO was ensured by the matching of the polished mating surfaces. In one case, a small amount of indium was melted and spread between these faces. Indium melts at 430 K, thus providing good thermal contact at high temperatures. In both cases, this temperature reading for the ZnO was verified using known TPD peak temperatures: 157 K for multilayer (three-layer) ice,[10] 590 K for simultaneous CO, CO_2, and H_2 evolution from HCOOH decomposition on sputter-damaged ZnO,[11,12] and, in one case, 300 K for multilayer cesium.[13] With or without the indium, the true temperature was about 25 K below the temperature read by the thermocouple, and this correction was applied to the temperatures reported here.

Copper was vapor deposited as described previously.[14] Dose rates were found to be reproducible to better than 10% from day to day, judging by XPS signals.

III. RESULTS

A. ISS, XPS, and LEED versus coverage

The adsorption of Cu on ZnO(0001)-O at 300 K has been previously studied by Campbell, Daube, and White[2] using XPS, Auger electron spectroscopy (AES), LEED, and He^+ ISS. We took limited data of a similar type at 300 K to verify that the present ZnO sample was behaving similarly, which indeed proved to be the case. We also took new uptake data at 130 K, which we wish to present here. A typical curve for the ISS and XPS signals versus Cu dose at 130 K are shown in Fig. 1. Since Cu and Zn are unresolved in ISS, the integrated intensity of their combined signals are reported here as "Cu + Zn." These data are qualitatively very similar to that reported previously at 300 K.[2] Both sets of data show a sharp break in the slope of the oxygen ISS signal versus dose, which must reflect a rather sudden increase in the probability that an incoming Cu atom will stop on top of previously deposited Cu atoms. Let us define N_1 as the copper coverage where this break occurs for the 130 K data.

The data points in Fig. 1 are not as close together as one would like for the accurate identification of this break point, but this was necessary to prevent beam damage by the He ions. Beam damage was proven to be negligible with the accumulated ion dose used here by repeating individual points on this curve at N_1 and $3N_1$, without intermediate ISS measurements. Since these control points fit well onto Fig. 1, and yet had far less cumulative ion dose, we can conclude that ion damage effects were negligible at least up to a coverage of $3N_1$. However, experiments such as that illustrated Fig. 1, which were taken with more closely spaced data points or with larger cumulative ion dose per point, showed observable differences due to beam damage by $3N_1$. Since the time required to do these single-point control experiments was also much less than that used for Fig. 1, the agreement also proves that impurity adsorption from background gases were negligible in Fig. 1. This was further confirmed by monitoring the TPD of possible background gases (CO, H_2O) following such uptake curves. The nearly linear decay in the oxygen ISS signal up to the break point, and the sharp change in slope there, were confirmed with control runs such as shown in Fig. 1, which did not extend to such high coverages but had more data points below $2N_1$. The fact that the percentage change in the ISS signals at the break point changed

by ~10% from run to run prevented us from compiling all these data into a single figure. It should be noted that the amount by which the oxygen ISS signal was attenuated at the break point N_1 in the uptake curve at 130 K (see Fig. 1) decreased somewhat with sample use. A sample that had been used for eight months in these studies showed an attenuation of only ~42%, compared to 55% for the newer sample in Fig. 1. The values for the signals at the break points quoted here are averages of several runs.

At 130 K, the oxygen ISS signal decreases by about 55% for the newer sample from its clean value at this sharp break point, compared to a smaller decrease by only about 35–40 % for the uptake curve at 300 K, also reported previously.[2] The sharp break in the substrate's oxygen ISS signal, seen here after $4\frac{1}{2}$ min of Cu dose, was originally interpreted in terms of a Stranski-Krastonov growth mode (monolayer completion followed by thick 3D islanding), where a monolayer was thought to be a complete or partially complete $p(1\times1)$ overlayer of Cu sitting in substrate lattice sites.[2] The Cu density of this (1×1) layer, if complete, would only be 1.1×10^{15} atoms/cm^2, or about 62% of the density of a Cu(111) plane (1.6×10^{15} atoms/cm^2). The residual oxygen signal in the He^+ ISS (a technique which is generally accepted to be sensitive only to the topmost atomic layer[15–17] was attributed to the possibility that He^+ ions could penetrate through the gaps between the widespread Cu atoms in a $p(1\times1)$ structure, and scatter off the oxygen ions beneath, without being neutralized.[2] The $p(1\times1)$ structure proposed in Ref. 2 was also consistent with the absence of any new LEED spots aside from the $p(1\times1)$ spots of the substrate, although background intensity measurements were not sufficiently accurate to rule out any disordered overlayer.

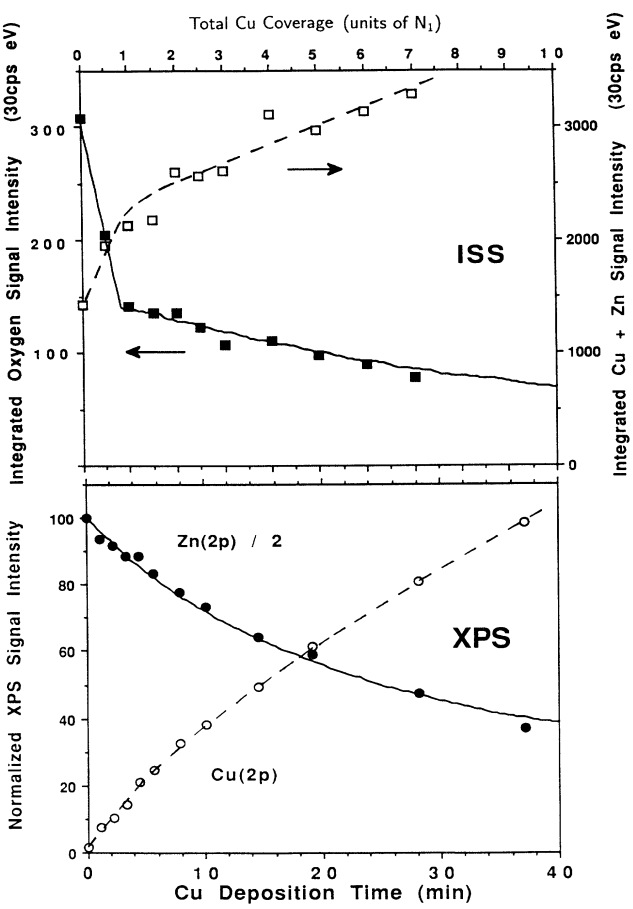

FIG. 1. Variations in the oxygen and (Cu+Zn) ISS intensities and the Zn($2p_{3/2}$) and Cu($2p_{3/2}$) XPS intensities with Cu deposition time onto ZnO(0001)-O at 130 K. The solid curves through the oxygen ISS and Zn($2p_{3/2}$) signals represent a simulated fit to the growth kinetics (see Sec. IV). The coverage N_1 corresponds to about 1×10^{15} cm^{-2} (see Sec. IV).

The scattering angle used here for ISS (135°) was different than that used in our previous study (120° Ref. 2), and the azimuthal orientation was also different. Thus the relative contributions of Cu and Zn to the "Cu + Zn" signal could be different here. Therefore, nothing definitive can be concluded from the differences in the relative change in this signal between zero Cu coverage and the break point in this curve.

We made new LEED observations at 130 K of a Cu coverage N_1 dosed at 130 K, which showed only the sharp $p(1\times1)$ spots of the substrate, but now with a very noticeable background increase compared to the clean surface. After a brief flash of this layer to 330 K (and recooling to 130 K), this new background LEED intensity decreased. This would be consistent with thermal ordering of Cu adatoms into larger or more tightly shaped $p(1\times1)$ domains. Alternatively, the decrease in the LEED background could be due to uncovering of the ZnO substrate as Cu atoms move into the second layer. As will be demonstrated by our ISS annealing studies below, such annealing does cause movement of about 25% of the Cu from the first layer into the second layer. However, the decrease in the background LEED intensity appeared to be substantially more dramatic than this. As observed previously,[2,3] Cu films of coverage exceeding about $6N_1$, which had been flashed to 360 K or above, or grown at 300 K, showed Cu(111) spots in addition to the substrate LEED spots.

B. Annealing behavior

Evidence that Cu atoms in the first layer start to move up into the second layer at 300 K was seen by monitoring the ISS spectrum versus annealing temperature for an initial coverage N_1 deposited at 130 K. The heating process used here was 5 K/s, followed by immediate removal of the heating power when the maximum temperature was reached. Thereafter, the sample cooled at about 5 K/s. The subsequent spectra were recorded at 160–130 K while cooling. These data are summarized in Fig. 2, which shows the integrated oxygen and Cu + Zn ISS signals versus annealing temperature. In no case did Cu leave the surface by desorption, as monitored by a mass spectrometer for temperatures up to 800 K. Thus the loss in Cu + Zn signal and the gain in oxygen signal upon annealing can only be attributed to redistribution of Cu in or on the ZnO. In a model where the oxygen signal

is proportional to the fraction of the ZnO surface area that is free of Cu, and the Cu+Zn signal is linearly related to the fraction covered with Cu, one would expect these two signals to be (scaled) mirror images of each other. Within the error bars of the data, this is the case. The starting surface at 130 K shows only about 40–55 % of the clean surface oxygen signal, depending on the age of the sample (see above), but this oxygen signal is regained upon annealing until, by 800 K, it reaches about 90% of the clean value. Thus, by 800 K, about 75% of the Cu that was originally visible in ISS is lost upon annealing because it becomes covered by other Cu atoms. This occurs in two stages. First, a relatively rapid change occurs at around 300 K, followed by a region of more slowly changing ISS signals above 380 K. Then the rate of change slowly increases with temperature, such that the slope at 700 K is again comparable to that in the steep region near 300 K. A brief report of similar behavior identified from the Cu/Zn AES ratio was reported previously.[18]

Similar behavior can be seen qualitatively in Fig. 3, which shows the ISS signals versus annealing temperature, in this case starting at 130 K with a Cu coverage of $7N_1$. Again, a rapid change occurs at ~300 K, followed by a slower region above 380 K. The only qualitative difference at this higher coverage is that the slope does not increase with temperature above 500 K. Both Figs. 2 and 3 indicate that the redistribution of Cu in/on ZnO occurs over a very broad temperature range. We will demonstrate that the ultimate result of this annealing process is to produce thick 3D Cu clusters which cover a smaller fraction of the ZnO surface.

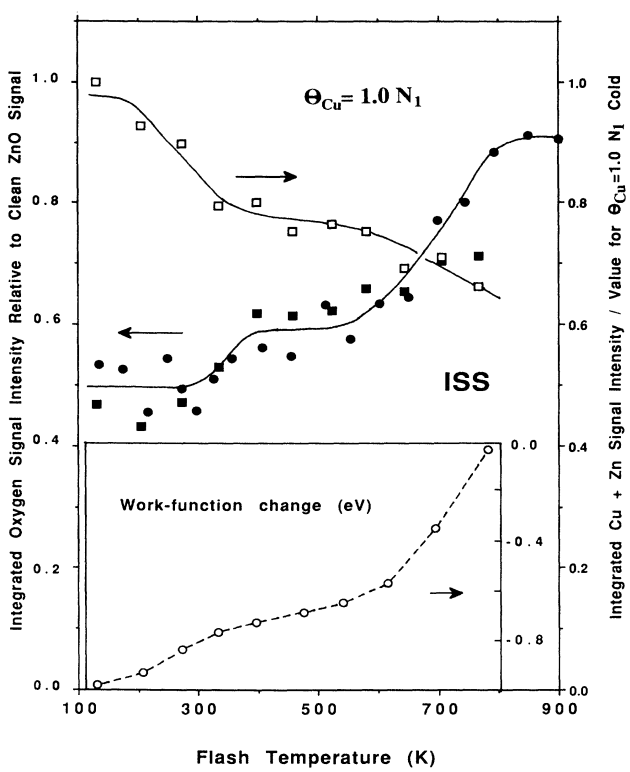

FIG. 2. Variations in the oxygen and (Cu+Zn) ISS signals with the temperature to which the film had been briefly flashed, starting with a Cu coverage N_1 deposited at 130 K. The square points represent a new sample, and the filled circles are for an older sample. Inset: The variation in the work function with the temperature to which the film had been flashed, starting with a Cu film of coverage N_1, deposited at 130 K.

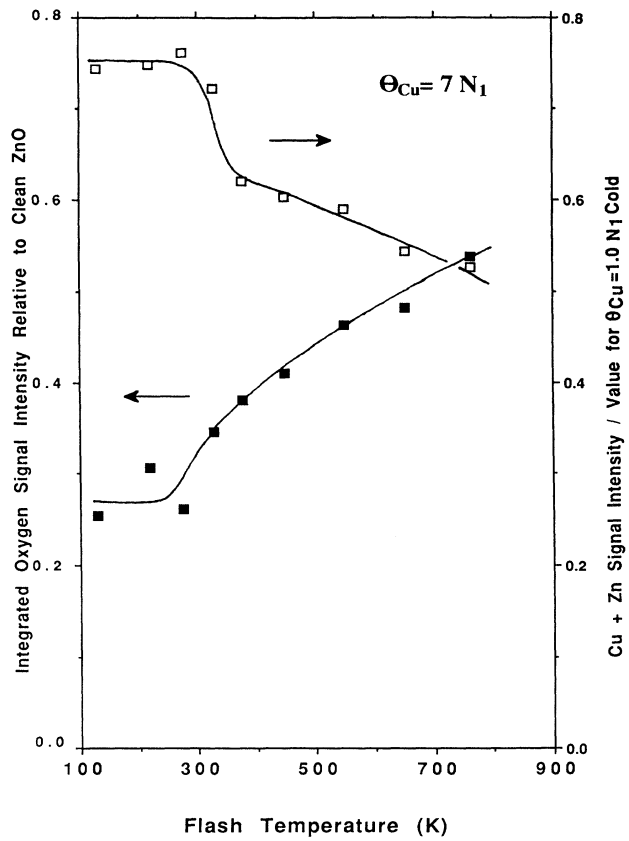

FIG. 3. Variations in the oxygen and (Cu+Zn) ISS signals with the temperature to which the film had been briefly flashed, starting with a Cu coverage $7N_1$ deposited at 130 K.

The history of the sample influenced the first step of this annealing process, which occurs at about 300 K, as can be seen in Fig. 2 by comparing data for a new sample (squares) with one eight months later (circles). The amount of clustering is more severe for the newer sample. The newer sample also showed a greater attenuation of the oxygen ISS signal upon dosing the Cu, so that the signal level reached at 400 K is the same in both cases. These differences between the old and the new samples were reproducible, since several such dosing/annealing experiments were performed in each case which revealed the same trends shown here.

C. Electronic structure of the Cu films

The electronic nature of these Cu layers were studied by XPS measurements of the Cu($2p_{3/2}$) core-level peak position and the Cu(L_3VV) XAES peak position, which

are presented as a function of annealing temperature in Fig. 4. The Cu film of thickness N_1 at 130 K has values for these which are closer to those reported for bulk Cu_2O than to bulk Cu (see boxes). The so-called "Auger parameter plus photon energy," which is just the sum of these XAES and XPS peak positions and thus cancels out charging and spectrometer zeroing errors,[19] is 1849.8 eV for Cu at coverage N_1 and 130 K. This is also much closer to the value of 1849.35±0.4 eV reported for Cu^{+1} in bulk Cu_2O than to the value of 1851.23±0.1 eV reported for bulk Cu.[19] However, these peak positions, especially for the XAES peak, are very dependent upon final-state relaxation effects.[19(b),20] Thus it is entirely possible that the Cu here is really neutral and metal-like in nature, but shifted toward lower kinetic energy (higher binding energy) because of ineffective screening of the final-state cations compared to bulk Cu whenever the Cu exists as a monolayer-thin film on ZnO. Such relaxation effects for XAES peaks are predicted to be three times the shift for a related XPS peak.[19(b)] A model where these peaks are due to zero-valent Cu but shifted from the bulk Cu values by final-state relaxation differences is consistent with the fact that the Cu(LVV) kinetic energy here is ~1.6 eV below that of bulk Cu. This shift is indeed about three times that of its Cu($2p_{3/2}$) peak, whose binding energy is only about 0.5 eV higher than bulk Cu.

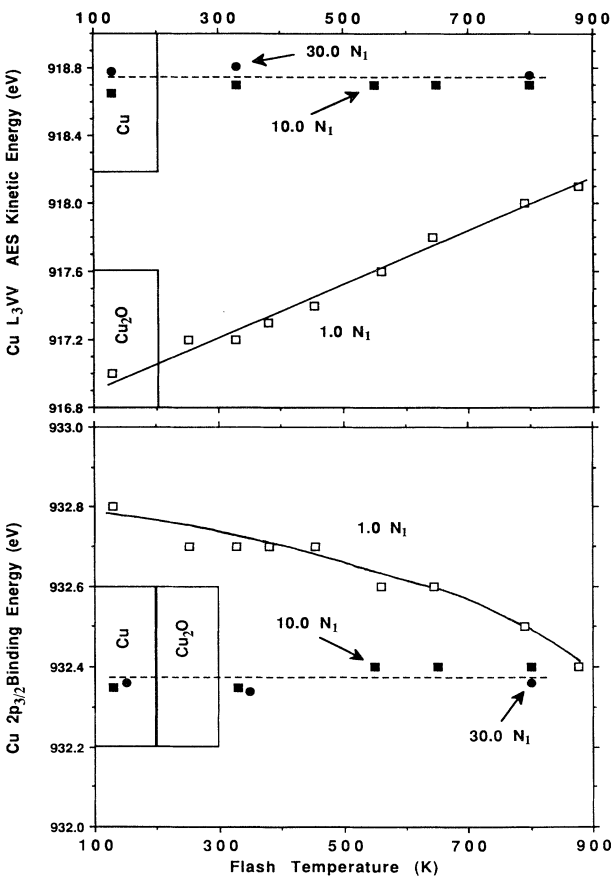

FIG. 4. Variations in the peak positions of the Cu(L_3VV) x-ray-excited AES peak and the Cu($2p_{3/2}$) XPS peak with the temperature to which the film had been briefly flashed, starting with films of Cu coverages $1.0N_1$, $10.0N_1$, and $30.0N_1$ deposited at 130 K. The boxes shown on the left axis reflect reported energies for bulk Cu and Cu_2O (Ref. 19).

As with the ISS signals, these XPS and Auger peak positions at $1N_1$ shift with temperature by 250 K, and continue to shift right up to 880 K. The Cu XPS and XAES peaks also end up at 880 K, being closer in energy to the reported values for metallic Cu than to those for Cu_2O. This would be consistent with an increase in the number of Cu nearest neighbors to Cu,[20] which accompanies thermally induced 3D clustering. That the values may still be slightly below the kinetic energy of thick Cu films or bulk Cu may simply be related to the fact that, at this low Cu coverage, the Cu particles are still not large enough even at 880 K to have full, bulklike relaxation of the final state.

Further evidence for the thickness of heavily annealed Cu clusters is revealed by their difficulty of removal by sputtering, compared to the relative ease of removing unannealed Cu layers. The residual Cu that remained after sputtering the annealed layers sufficiently long to have cleaned an unannealed Cu layer of the same coverage showed Cu peak positions and line shapes close to metallic Cu, but quite different than reported values for Cu^{2+} or Cu^{1+}.[19] Upon annealing this sputtered Cu/ZnO surface to 850 K to restore a good LEED pattern, this residual Cu, which was quite thick but which covered only a tiny fraction of the surface, showed no tendency to respread across the surface, according to unchanged XPS and ISS intensities. It remained as metallic 3D clusters, as judged by peak positions in XPS and XAES. This shows that Cu does not have a thermodynamic driving force to spread even in one monolayer across ZnO(0001)-O. That it spreads as well as it does during deposition at 130 K must be a dynamical effect, as we will discuss below.

The electronic nature of the Cu is further revealed by measurements of the work-function and band-bending changes which accompany Cu adsorption at 130 K. The band bending is measured by following the shift in substrate core levels with respect to the Fermi level (spectrometer reference)[21] as a function of the Cu dose, as shown in Fig. 5 along with the work function change. The bands, which are bent upward on the clean surface,[22] are bent back downward upon Cu adsorption. The work function simultaneously decreases. Interestingly, the major effect of Cu occurs in the first $0.07N_1$, which is a tiny fraction of a monolayer. Similar changes at very low coverages are frequently observed in metal deposition on semiconductors, i.e., in Schottky-barrier formation.[24,25]

The solid dots in Fig. 5 show the change in the position of the valence-band maximum with respect to the vacuum level, which is obtained by subtracting the band-bending effect from the work-function change.[21] This change directly reflects changes in the local surface dipole,[21] so it can be interpreted in the same way that adsorbate-induced work-function changes are interpreted on metallic surfaces. The initial sharp decrease in this lo-

cal surface dipole, and the simultaneous downward band bending, between zero coverage and $0.07N_1$ is consistent with the donation of Cu electrons to the substrate's depletion layer, to make cationic Cu species.[21,24] However, this curve nearly stops decreasing above $0.25N_1$ in coverage, proving that the Cu adatoms are going down as nearly neutral, unpolarized species. This is also consistent with the almost complete lack of band bending and work-function change for coverages between $0.25N_1$ and $1N_1$. Thus the vast majority of the first monolayer of Cu is neutral, after the first few percent, which are cationic.

When this surface at a Cu coverage of N_1 and 130 K is heated, its work function increases back toward the clean surface value, as shown in Fig. 2 (inset). This would be consistent with the ISS results (Fig. 2), which showed that such heating uncovers more and more of the clean ZnO surface as the Cu agglomerates into thicker islands. The temperature dependence of the work-function change is also qualitatively similar to the ISS signals, with a fast region between 200 and 350 K, followed by a slow region above 380 K, and finally an acceleration to 750 K. Apparently, even the first few percent of a monolayer of cationic Cu, which gave rise to the dramatic work-function change and band bending of Fig. 5, is not even thermodynamically stable relative to Cu in thick 3D metallic islands. Otherwise, the work function after annealing would remain at the value of 0.8 eV below the clean surface value characteristic of this initial cationic Cu (see Fig. 5). The area-averaged work function, which we measure here, is dominated at 780 K by large areas of clean ZnO(0001)-O, with contributions from a smaller fraction of the surface ($\sim$20%, see above) which is covered by thick metallic Cu. Since the thick Cu patches have (111) orientation according to LEED,[2] their work function is only $\sim$0.5 eV below the clean ZnO value.[8] Thus a work function of $0.2\times0.5=0.1$ eV below the clean surface value is predicted, following an 800 K anneal which is within 0.1 eV of the observed result in Fig. 2 (inset).

D. Angular-resolved XPS measurements of film structure

Further evidence concerning the structure of these Cu films was provided by angular-resolved XPS measurements. The clean ZnO surface showed a strong angular variation in the Zn($2p_{3/2}$) and O($1s$) XPS intensities, as shown in Fig. 6, with major peaks at about 0°, 33°, and 56° and 0°, 24°, and 40°, respectively, which can be attributed to the forward focusing (searchlight) effect.[26] The expected angles for forward focusing of Zn and oxygen core-level electrons are shown as the solid and dashed arrows, respectively, in the inset of Fig. 6. Here the model

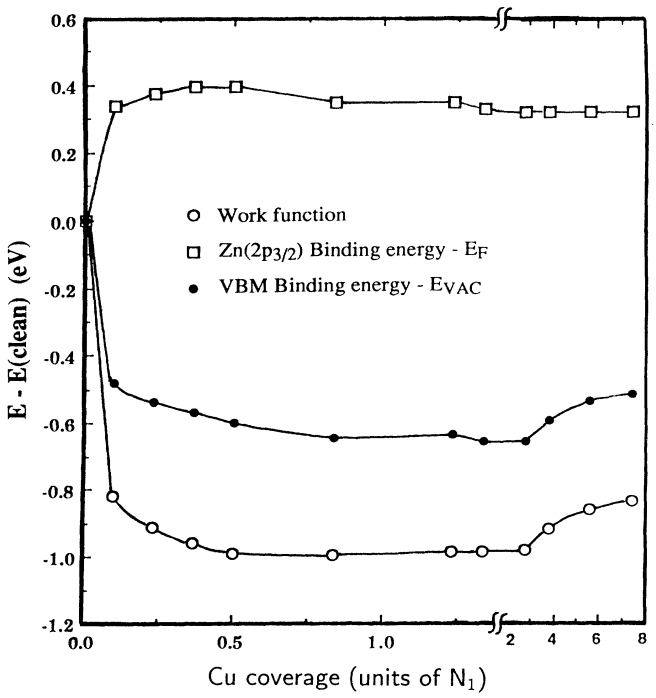

FIG. 5. Variations in the work function and the binding energy of the Zn($2p_{3/2}$) peak with respect to E_F with Cu coverage during deposition at 130 K. The latter value reflects the long-range Cu-induced band bending. Also shown is the difference between these two curves, which gives the Cu-induced shift in the position of the valence-band maximum (VBM) relative to the vacuum level (E_{vac}), since all the bands shift together. The latter directly reflects the local dipole layer due to adsorbed Cu.

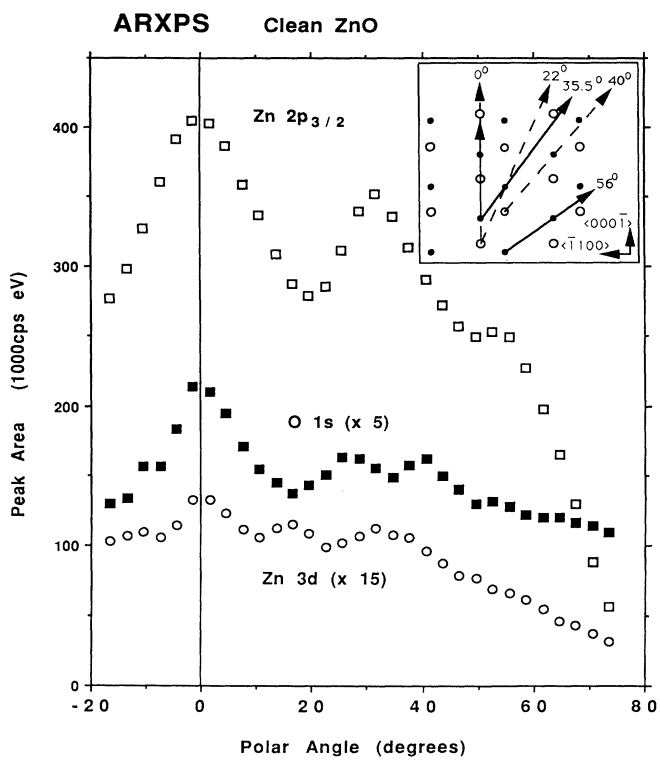

FIG. 6. Variation with polar angle along the $\langle\bar{1}100\rangle$ azimuth in the integrated intensities of the Zn($2p_{3/2}$), O($1s$), and Zn($3d$) XPS peaks for the clean ZnO(0001)-O surface. The arrows in the inset show the angles where forward focusing peaks are expected for O (dashed) and Zn (solid), based on the bulk structure, neglecting all except the strongest scattering neighbors (see text).

is quite simplified in that we ignore focusing by oxygen (since it is a weak scatterer compared to Zn) and by neighbors that are more than 6 Å away. Contributions from these weaker effects probably cause the observed peaks to appear at slightly different angles than predicted by this model in some cases, but the overall agreement is quite good. The Zn($3d$) peak showed similar angular structures to the Zn($2p_{3/2}$) peak, with an additional peak at about 17° (see Fig. 6). This peak cannot be attributed to forward focusing from a Zn core location, but it arises from a valence level ($\sim$10 eV B.E., binding energy) which may have a very noncorelike spatial extent. The angular distributions of the O($1s$) and Zn($3d$) electrons were also measured in the azimuth perpendicular to the $\langle 11\bar{2} \rangle$ direction, and showed strong structure as well. Those distributions are harder to interpret because of the lower symmetry there, so they are not presented here.

These variations in the O($1s$) and Zn($3d$) signals were unaffected by the deposition of a coverage N_1 of Cu at 130 K, except for a uniform attenuation of the signals by $\sim 10\pm2\%$ and $12\pm4\%$, respectively, independent of angle out to 60° within these error bars. The absence of forward-focusing effects due to the Cu film would be consistent with an overlayer in poor registry with substrate sites. However, it is unclear whether a single half monolayer of Cu in registry with the ZnO would significantly alter these distributions, which arise from rather deep within the sample. The Cu($2p_{3/2}$) signal for this layer also showed no significant angular variation other than that due to the instrument response, except for a broad maximum at about 0°, as shown in Fig. 7(a). The smooth increase in Cu signal going to the right in this figure is due to the fact that more of the sample surface fits within the narrow (2-mm) focusing region of the analyzer slits. This is finally counterbalanced and overcome by the fact that the sample moves out of the analysis region at very large angles ($>60°$), since it is not mounted exactly on the axis of rotation. If the sample surface were perfectly mounted on this axis of rotation, the Cu signal for submonolayer, disordered Cu would be expected to increase as $1/\cos\phi$ up to 90°. Thus no real angular variations occur in the Cu signal, except for a broad peak at 0°. The absence of peaks due to forward focusing at angles between 20° and 50° is consistent with the Cu being in a single-monolayer film, as we proposed above, since there is nothing above it to cause forward focusing.[26] The broad peak at 0° is not likely, due to forward focusing of Cu electrons by Cu, since any reasonable stacking structure for Cu on Cu that gave a peak at 0° would require the Cu to be at least three layers thick, which is inconsistent with the XPS and ISS intensities at this coverage (see Sec. IV). This 0° peak might be attributed to constructive interference from the outgoing Cu photoelectron wave, which is backscattered off Zn atoms below. This would require some degree of registry between the Cu and the ZnO lattice.

The angle-resolved XPS also gives evidence concerning the surface structure after annealing this Cu film briefly to 370 K. Figure 7(b) shows the resulting Cu signal versus angle, for comparison to the Cu signal from the unannealed film at coverage N_1. First, a loss of Cu from the topmost plane is obvious in the $\sim$5% loss in XPS signal at all angles. This is consistent with the ISS results of Fig. 2, which show that about 30% of the Cu moves up into the second layer by the time this temperature is reached. The angular distribution has otherwise not changed significantly. No new structure is observed which might be attributed to forward focusing of photoelectrons from the first layer of Cu by Cu atoms in the second layer. The absence of new forward-focusing peaks is probably due to the disordered nature of the adlayer, which could give an unresolved superposition of broad forward-focusing peaks at many different angles, depending on the local arrangement of Cu atoms on the ZnO substrate.

Curves c and d of Fig. 7 show the angular distributions of Cu($2p_{3/2}$) electrons from a layer of coverage $2N_1$ grown at 130 K, and flashed briefly to 370 K, respective-

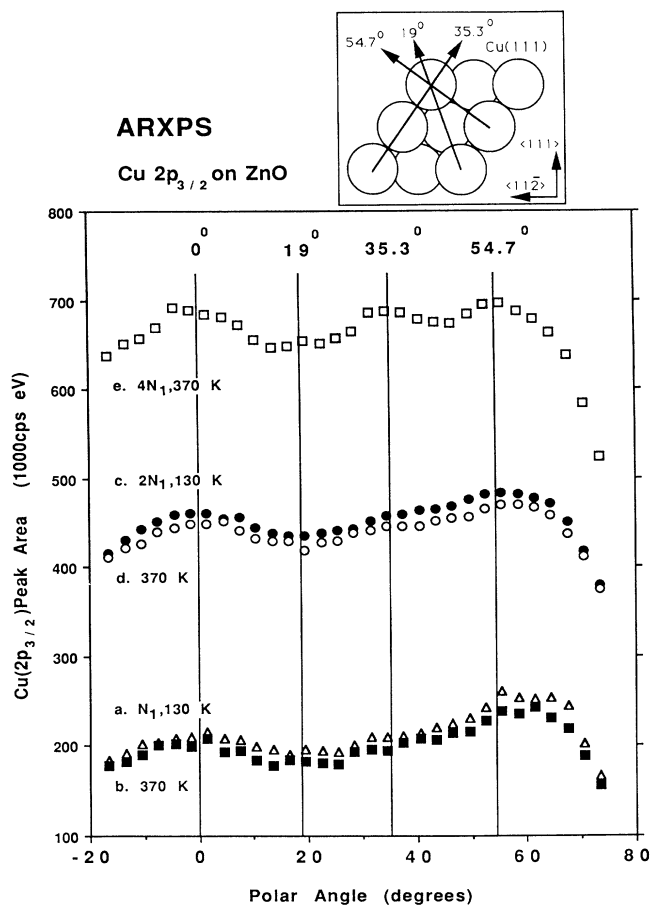

FIG. 7. Variation with polar angle along the ZnO $\langle \bar{1}100 \rangle$ azimuth in the integrated Cu($2p_{3/2}$) XPS intensity for the ZnO(0001)-O surface after (a) dosing coverage N_1 of Cu at 130 K; (b) flashing this surface briefly to 370 K; (c) dosing coverage $2N_1$ of Cu at 130 K; (d) flashing this surface briefly to 370 K; and (e) dosing coverage $4N_1$ of Cu at 130 K and flashing briefly to 370 K. The arrows in the inset show the angles where forward focusing peaks are expected for a Cu(111) film azimuthally oriented with respect to the ZnO, as observed in LEED at higher coverages.

ly. The effect of the instrument response function between 0° and 60° is now partially counterbalanced by the attenuation of Cu electrons by Cu above, which is more serious at larger angles. This leads to a much flatter distribution in this region. Again, the only obvious structure in either the 130- or the 370-K distribution is the peak at 0°, except perhaps a weak new peak at 35°. Again, the signal intensity decreases by ~4% after the flash to 370 K, indicating movement of Cu onto Cu to make thicker, smaller islands.

Finally, curve *e* of Fig. 7 shows the distribution for a coverage of $4N_1$ which had been flashed to 370 K. This thicker layer begins to clearly show Cu(111) structure, with new peaks at 35° and 55°, and perhaps a weak peak at 19°. As shown by the inset in Fig. 7, these peaks can all be attributed to forward focusing of Cu electrons by Cu in a Cu(111) structure, azimuthally oriented to the ZnO as shown in prior LEED studies at higher coverage,[2] whereby the Cu$\langle 11\bar{2}\rangle$ azimuth is parallel to the ZnO$\langle \bar{1}100\rangle$ azimuth. The Cu(111)-like LEED structure only begins to appear at somewhat higher coverages, since it requires long-range order. The peak at 0° may be due to some HCP-like stacking of the Cu layers.

IV. DISCUSSION

A. The structure of submonolayer Cu films

An issue of central importance here is the structure of the Cu overlayer at coverages below N_1 in Fig. 1. Our work-function and band-bending measurements clearly show this Cu to be largely neutral in charge. This conclusion is consistent with the results of resonance photoemission measurements by Didziulis *et al.*[3] on this same system. It seems unlikely that an isolated Cu adatom bonded only to oxygen ions of the ZnO(0001)-O surface would remain neutral and unpolarized. This intuition is confirmed by quantum-chemical calculations of cluster models of this system, which showed that isolated Cu adatoms should have a charge like that of Cu cations in bulk CuO.[27] Thus Cu could only stay neutral on this surface by taking on Cu nearest neighbors in a metal-like 2D film. Perhaps a better way to make this argument is simply to restate that the data prove that the Cu atoms are neutral, and recognize that neutral Cu atoms are well known[28] to have strongly attractive Cu-Cu interactions on surfaces, which will drive them together into at least 2D islands unless there is a strong preference for specific sites on the surface. There does not seem to be a strong preference for specific sites, since LEED shows no evidence for an ordered overlayer at N_1. Increasingly, data show that metals like Cu have very low activation energies for diffusion on metal oxide surfaces. For example, Cu clusters into thick 3D islands which cover only a tiny fraction of the surface at 160 K on a TiO_2(110) surface, which terminates in mostly oxygen.[17] Palladium on this same ZnO surface also clusters into 3D islands, which also cover a tiny fraction at the surface of 300 K.[29] Furthermore, even the weak attractions between noble-gas atoms give rise to 2D islanding on metal oxides at adatom-adatom spacings which do not match the substrate sites.[30,31] Thus one might expect a very noncorrugated interaction potential for neutral Cu adatoms along the oxide surface, which would favor 2D islanding at nearly the metallic Cu-Cu distance.

Further evidence to support a structural model where the first Cu layer is located in 2D metal-like islands can be found in the surface's chemisorption behavior, which we report elsewhere: This surface shows thermal desorption spectra for CO (Ref. 6) and H_2O,[7] and XPS spectra for adsorbed CO,[6] which are nearly identical to those for Cu(110). Furthermore, adsorbed formate on these films decomposes at the same temperature as on Cu(110).[32] Finally, the valence-band photoemission spectra for submonolayer Cu films on this surface show a very delocalized Cu(4*s*) peak even at much lower coverages.[3] We therefore conclude that the Cu forms metal-like islands up to the coverage N_1, even at 130 K. That these are 2D rather than 3D islands (i.e., only one layer thick) and only cover about 45–55 % of the surface will be proven by quantitative analysis of the ISS and XPS uptake curves below. This is also obvious from the very nonbulklike XAES position for this Cu film (Fig. 4), which changes to a bulklike value after annealing.

Whether these Cu islands are in some registry with the ZnO below is still not completely clear, although the peak at 0° in the Cu($2p_{3/2}$) distribution (Fig. 7) suggests some registry. A $p(1\times1)$ structure with two Cu atoms per unit cell, one above the Zn ions nearest the surface and one in the threefold hollow sites of the surface oxygens, would provide for three Cu nearest neighbors to each Cu atom. This would not be consistent with its metal-like character, and would explain this 0° peak if the Cu to Zn distance were proper for constructive interference. It would also be consistent with the LEED observations, as well as the magnitudes of the XPS and ISS signals (see below).

The dramatic band-bending and work-function changes reported for tiny Cu doses at 130 K in Fig. 5 agree qualitatively with the results measured for this system at 300 K by Didziulis *et al.*[3] However these values stay nearly constant beyond the first 7% of a monolayer in our data, whereas they moved back by 0.3–0.4 eV toward the clean surface values as the coverage increased to a monolayer in the data of Didziulis *et al.*[3] This can mostly be attributed to the temperature difference, since the work function increases by about 0.25 eV over this temperature range at coverage N_1 (Fig. 2, inset). Also, the magnitude of the initial work-function decrease was about 0.5 eV larger in our data, probably due to the fact that our clean surface had a work function that was about 0.5 eV higher. Since the Fermi level is probably close to the bottom of the conduction band in the bulk of either sample,[5,9] the difference in clean surface work functions implies that our clean surface had more upward band bending, as do vacuum-cleaved samples.[9,22] Such upward band bending arises from the depletion layer created by electron donation from oxygen vacancy levels near the conduction band into acceptor-type surface states. The position of these surface states in the band gap determine the magnitude of this band bending.[5]

B. A kinetic model for film growth

Taken together, uptake curves such as those shown in Fig. 1 which combine XPS and ISS data offer a very rich

picture of the growth structure. Many models which would be consistent with either set of data individually are ruled out by these combined data. In interpreting these XPS data, we tried electron inelastic mean free paths λ for the Zn($2p_{3/2}$) line excited by Al($K\alpha$) x rays in the range 8–15 Å, based on the range of values expected from the literature for these 465-eV electrons.[33] We assumed that the substrate (oxygen) ISS signal was proportional to the fraction of the ZnO surface that is free of Cu. This assumption is based on Refs. 15–17. However, it has been shown that the He^+ neutralization probability increases strongly as the work function decreases in the case of Cs on Cu(110).[34] In view of the large Cu-induced work-function decrease here (Fig. 5), this assumption could be questioned. However, the substrate ISS signal was proved to decrease very little for the thin Cu coverages ($0.07N_1$) needed to bring about this large work-function decrease, showing that the neutralization probability is not strongly affected here by this work-function change. This may be due to the very low Cu coverage, which means that the distance between these dipole centers is large, and the probability of a He ion striking near enough to this Cu center to be neutralized is small. The islanding which occurs in the adlayer helps to keep this assumption about ISS intensities valid at higher coverage.

The rapid, but incomplete, initial attenuation of the oxygen ISS signal severely restricted the types of models that could fit the data. In any layer-by-layer or in any Stranski-Krastanov model, this signal dies at the completion of the first monolayer (provided the Cu is nearly close packed, for which we argued above), which is not observed. This signal dies too rapidly at short times for any Volmer-Weber model. To accurately model the complex growth behavior seen here, we were forced to simulate the growth kinetics within a stochastic model. In these simulations, Cu atoms were deposited one by one onto a ZnO surface which had an area sufficient to accommodate 10 000 atoms per layer, but with no specific sites. Within each layer, the Cu atoms were assumed to cluster into 2D islands. The fractional Cu coverage in layer i was defined as θ_i (= the number of Cu atoms in layer i divided by 10 000). For convenience, the substrate was defined as layer zero, and θ_0 was set to 1.0 at the start of the simulation, with θ_i equal to zero for all other i. Each new incoming Cu atom was assumed to make its initial contact with the surface, or "hit" the surface, in some layer i. The probability that an atom hit in a layer i is proportional to θ_{i-1}-θ_i, where θ_i is the fractional coverage of layer i. Random numbers were generated by computer to decide upon all branching probabilities. We first tried a "hit and stick" model, where the Cu atoms stick in the layer where they hit. In this model, the substrate ISS signal died too slowly in the early stages of growth, and too rapidly later. Clearly, something else is occurring which makes the atoms spread better at short times, but which induces 3D clustering at long times. Let us treat the problem of spreading at low temperatures first.

There is an effect observed in metal growth on the same metal[35,36] which is of importance in understanding this. Whenever there are monolayer-thick islands covering only part of the surface, and a new atom hits on top of one of those islands, it would energetically preferable to drop the layer below and bond to the edges of islands. The energy difference is just the energy of 2D evaporation from the island edge, E_i, since an isolated adatom in that case has the same energy in either layer. This new atom therefore frequently moves down to the edge of 2D islands in the layer below. This occurs with unit probability by thermal migration at high enough temperatures, provided islands have not yet nucleated on top of that layer.[35] At low temperatures, the energy barrier for migration can be overcome dynamically by using part of its adsorption energy.[36] In either case, the probability of such "down stepping" into the layer below falls off abruptly as the island size in the layer below (or coverage, for a fixed number of islands) increases beyond a certain critical value.[35,36] (If this size and the down-step probability are large enough, ideal layer-by-layer growth results.[36]) In order to simulate this type of effect in an approximate way here, we modified the hit-and-stick model by assuming that an adatom hitting in layer $i+1$ would descend to the layer i below with a probability p_i, which drops to zero whenever the coverage in the layer below exceeds a critical value, $\theta_{cr,1}$. These two parameters were assumed to be the same for all layers. Such a model, with $p_i=1.0$ and $\theta_{cr,1}=0.54$, allowed us to simulate the 130-K data with good accuracy up to the break point in the ISS signal, but the substrate ISS signal still died much too rapidly above that point. Clearly, the first monolayer of Cu was continuing to populate too rapidly beyond coverage N_1 if the Cu atoms which hit in clean ZnO patches were allowed to stay in that first Cu layer.

In order to simulate the very slow decay in the substrate ISS signal beyond the break point, we had to add a feature to the model which allowed Cu atoms hitting on clean ZnO sites to migrate up onto existing Cu islands. This must, however, be precluded at low coverage or the initial, steep decay would not be properly modeled. Thus we performed simulations identical to that described above, with an important additional assumption: Cu atoms going into any layer were assumed to move into the layer of Cu above it with probability p_{up}, provided the Cu coverage in that "upper" layer exceeds some critical value θ_{min}, but does not yet exceed 90% of the coverage in the layer below. Actually, there is a very compelling physical basis for such an assumption, as we will explain below. The results of this simulation are presented as the solid lines through the data in Fig. 1, which fit the ISS and XPS data very well. The parameters used in this model are $p_i=1.0$, $\theta_{cr,1}=0.54$, $p_{up}=0.9$, and $\theta_{min}=0.01$. The mean free path of the Zn($2p$) electrons was taken to be 3.81 times the thickness of a one-layer-thick Cu island. If these islands have a packing density like Cu(111), or 1.77×10^{15} cm^{-2}, this layer thickness is 2.1 Å, making $\lambda=8$ Å. If the Cu atoms are packed with two per ZnO unit cell, the layer thickness is 2.61 Å, making $\lambda=10$ Å. These are both within the acceptable range (8–15 Å, see above). The coverage N_1 corresponds to 0.96 and 1.19×10^{15}, respectively, for these two packing densities.

To help show the structure generated by this growth model, in Fig. 8 we have plotted the coverage of each layer versus dose time as predicted by this model. Note that this model displays certain features of both the Volmer-Weber and layer-by-layer mechanisms in that clusters form which do not cover the whole surface, yet the clusters themselves grow in a flat, layer-by-layer way.

Let us make a more quantitative estimate of the thickness of these 2D islands using the results of the angular-resolved XPS measurements from Sec. III D. There we showed that the attenuation on the Zn($2p$) peak area by a coverage $1N_1$ of Cu at 130 K was 12%, averaged over the polar angles from 0° to 60°. That of the O($1s$) peak was 10%. Let us assume these attenuations to be due to a layer of thickness t which only covers 55% of the surface, based on our ISS results. If we use the mean literature values of electron mean free paths for these peaks of 11.5 and 17 Å, respectively, from Ref. 23, the island thickness t must be 2.2–2.6 Å. This compares to a thickness of 2.1 Å for a single layer of Cu(111). A greater packing density could be due to the natural buckling that would result from the Cu film trying to follow the geometric corrugation of the substrate.

Our annealing and sputtering experiments prove that the surface thermodynamically prefers the Volmer-Weber mode of 3D clustering. The growth depicted in Fig. 8 is thus a result of the dynamical effects necessary in the model, and not thermodynamics. As evidenced by the ISS signal versus temperature (Figs. 2 and 3), 3D clustering is kinetically disallowed at 130 K, and becomes allowed only at 280 K and above. This would seem to be direct contradiction to the model depicted by Fig. 8, which requires substantial 3D growth before monolayer completion even at 130 K. However, as we will show below, Cu atoms coming from the gas phase nucleate on the topmost layer and create a pathway for atoms in lower layers to move up into that top layer with a lower activation barrier. The annealing experiments of Figs. 2 and 3 do not have the continuous supply of these freshly deposited Cu atoms and the new islands they create, so the activation energy is much higher for Cu to make thicker islands, as we will show.

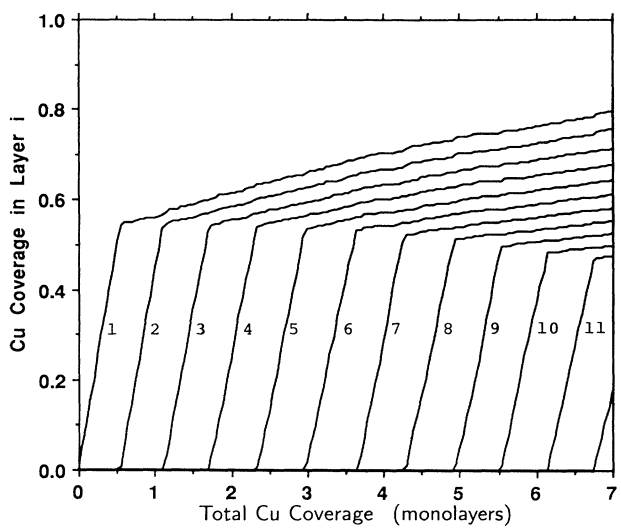

FIG. 8. The Cu coverage in each layer i as a function of the total Cu dose at 130 K, as predicted by the growth model which we used to fit the data of Fig. 1. As can be seen, the first layer fills to ~50% of completion (with 2D islands). Subsequently, most of the new Cu goes on top of these islands, while the island size or number increases only slowly. The parameters used in this model are as follows: $p_i=1.0$, $\theta_{cr,1}=0.54$, $p_{up}=0.9$, and $\theta_{min}=0.01$. (see Sec. IV B for a description of these parameters.) The model is very insensitive to the choice of island diameter, which was taken to be 40 Cu atoms here.

C. A plausible energetic model to explain the growth kinetics

We will now describe the energetics which are indeed expected for this system, and which naturally give rise to these curious growth rules needed to simulate the uptake data of Fig. 1, yet do not violate the annealing data of Figs. 2 and 3. The top part of Fig. 9 shows a small hypothetical part of the surface containing an island of Cu built up to three monolayers in thickness. The bottom part of the figure shows qualitatively what we expect the energy to be for the next Cu atoms as it diffuses along this surface. We assume for simplicity that the energetics in the second layer and beyond are identical, although certain differences are implied by the absence of Cu(111) LEED spots until several layers thickness. Since 2D islands are readily formed at 130 K, the barrier for Cu diffusion over ZnO is taken to be very small. The barrier for diffusion along the Cu terraces is assumed to be small and easily accessible at 130 K.[37] The magnitudes of these diffusion barriers in the figure should not be taken literally, but only as an indication that these steps are rapid.

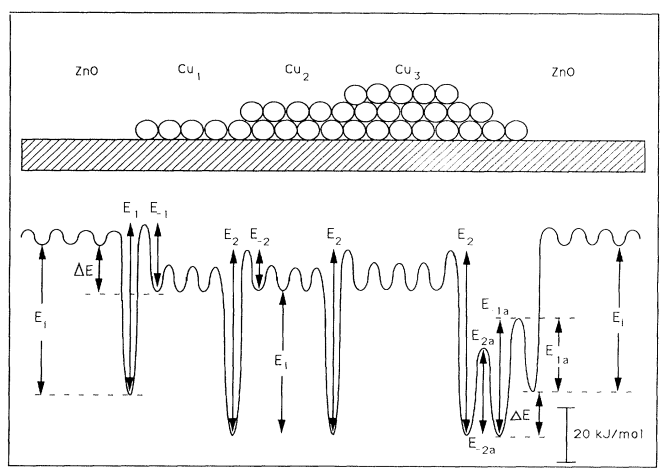

FIG. 9. Top: Schematic side view of the ZnO(0001)-O surface with a hypothetical Cu island of three-layer thickness. Bottom: Energetic diagram showing the magnitudes of the energy barriers that would be experienced by another Cu atom as it diffused along this surface, up onto this Cu island, and back down again. The magnitudes of the barriers were determined as described in the text to be $E_i=53$, $\Delta E=16$, $E_1=61$, $E_{-1}=24$, $E_2=66$, $E_{-2}=13$, $E_{2a}=E_{-2a}=31$, $E_{-1a}=42$, and $E_{1a}=26$, all in kJ/mol. This model describes well the observed growth and annealing kinetics.

The 2D evaporation energy for a Cu atom to detach itself from an island edge and move out alone onto a Cu terrace is about 53 kJ/mol,[40] shown as E_i in the figure. This energy arises from the loss of Cu neighbors and their attractive interactions. The barrier (E_{-2}) for an isolated adatom on a Cu terrace to step down over the edge of an island onto the edge of an island below is about one fourth of this value,[41] or 13 kJ/mol, making the barrier for an up-step (E_2) about $53+13=66$ kJ/mol. The thermodynamic tendency for Cu to cluster into 3D islands at high temperature certainly shows that Cu on Cu is more stable than Cu on ZnO (i.e., ΔE in Fig. 9 is positive). Adsorption of CO seems to induce a redispersion of Cu bilayers on this surface at 130 K,[6] which implies that Cu on Cu is more stable than Cu on ZnO by an amount which is less than the heat of adsorption of CO, or about 50 kJ/mol.[6] A Cu atom on ZnO was therefore assumed to be about $\Delta E=16$ kJ/mol less stable than an equivalent Cu atom on a Cu layer. The energy ($E_i=53$ kJ/mol) required to move an atom from an island edge to a terrace is assumed to be independent of whether this occurs on ZnO or Cu, since this energy arises from lateral Cu-Cu bonding. The barrier E_{-1} is similar in physical structure to E_{-2}, and it is assumed to differ from E_{-2} by about two thirds of the difference in reaction energies (ΔE) between these two steps, based on typical linear-free-energy relationships.[42] Thus $E_{-1}=13+16\times\frac{2}{3}=24$ kJ/mol. E_{1a} is estimated in an identical way from E_1 and E_i to be 26 kJ/mol. Also, E_{2a} is estimated from E_2 and E_i to be 31 kJ/mol in the same way. The barrier E_{-1a} is just $\Delta E+E_{1a}=16+26=42$ kJ/mol, by definition (see Fig. 9). Similarly, E_1 is just $E_i-\Delta E+E_{-1}=53-16+24=61$ kJ/mol, by definition.

Thus all of the energies of Fig. 9 are fully established. They are admittedly very approximate, but nevertheless reasonable and consistent with current knowledge of this system. Our goal here is only to show that the growth rules we imposed in our model above are a natural consequence of perfectly reasonable energies, and that these same energetics can explain the annealing behavior and the CO-induced redispersion of Cu bilayers. Let us now explore those consequences. Later, we will show that the growth kinetics are rather insensitive to most of these exact energy values, but that certain features of this energy diagram are rather critical.

First, it is useful to consider which of the energy barriers of Fig. 9 are easily accessible at 130 K, and which steps are kinetically prohibited. Assuming a preexponential factor of 10^{13} s^{-1}, a step with an activation barrier of 32 kJ/mol gives a jump rate of one per second at 130 K. Thus all steps with lower barriers should be quite rapid on the time scale of Fig. 1. This includes *every* step in Fig. 9 except those with barriers E_1, E_2, and E_{-1a}. Most critical here is to recognize that unassisted up-steps (E_1 and E_2) have barriers greatly in excess of 32 kJ/mol, so they will be kinetically prevented. Also, E_i is large so that 2D evaporation will also be precluded at 130 K, though this is not critical to our model. The largest part of barriers E_1 and E_2 comes from this 2D evaporation energy E_i, however, and it is critical that E_1 and E_2 be kinetically precluded at 130 K. Otherwise, the system would show strong 3D clustering even at 130 K.

Clearly, in Fig. 9, a Cu atom at the edge of an island on ZnO is more stable than an isolated Cu adatom on a Cu terrace. Thus there is an energetic driving force of $E_i-\Delta E=37$ kJ/mol for a lone Cu adatom in layer 2 to descend to the edges of Cu islands in the first monolayer *before* islands of the second layer start to nucleate. This is also kinetically possible at 130 K, since the barrier $E_{-1}=24$ kJ/mol is so small. These two features lead to efficient 2D spreading. Once islands exist in the second layer, a Cu atom will be more stable at the edges of such islands than at the edges of islands on the ZnO itself by $\Delta E=16$ kJ/mol, and this efficient spreading will cease. Nucleation of islands in the second layer will occur above a certain critical island size (or coverage in layer 1, assuming a fixed number of islands). A similar conclusion was reached by the Comsa group to describe He diffraction studies of Pt growth on Pt,[35] and by the Behm group recently to describe scanning tunneling microscopy (STM) observations of Au growth on Ru.[43] Their explanation for this had to do with the limited diffusion rate across terraces, but we believe it can occur even at quasiequilibrium (i.e., when terrace diffusion is so fast that there is no concentration gradient across a terrace). This can be shown by estimating the steady-state coverage θ_2 in layer 2 of the Cu while it is still in very low concentration in that layer as a 2D lattice gas. By equating the deposition rate into that layer ($=FA\theta_1$ where F is the flux, and A is the sample area) with the rate of migration down from layer 2 into layer 1 ($=k_{-1}P\theta_2/\theta_1$, where k_{-1} is the rate constant over barrier E_{-1} and P is the island perimeter), we can estimate θ_2:

$$\theta_2=FA\theta_1^2/(k_{-1}P) .$$

Since the island perimeter will grow like $\theta_1^{1/2}$ for a fixed number of compact islands, the fractional coverage of layer 1 by adatoms in layer 2, θ_2/θ_1, will increase as $\theta_1^{1/2}$. In all systems, condensation (island formation) occurs at equilibrium above some critical concentration, $(\theta_2/\theta_1)_{cr}$. Thus we expect island formation in layer 2 to occur only above some critical coverage in layer 1, $\theta_{1,cr}$. We have mimicked this effect in our simulations by having atoms descend to the layer below with unit probability until θ_1 exceeds $\theta_{1,cr}$, above which they stay in the second layer if they hit there, stuck to the edges of islands. We set $\theta_{1,cr}$ to 0.54 to fit the data.

Let us now consider such island nucleation on thicker islands. The main difference in the kinetics here is that the down-step barrier ($E_{-2}=13$ kJ/mol) is substantially smaller than E_{-1} (24 kJ/mol), so that k_{-2} will be much larger than k_{-1}. Thus the steady-state concentration of 2D gas (θ_3, for example) will be lower in these higher layers than in layer 2, for islands of the same size. Since the 2D condensation energy E_i is the same in all layers, the critical island size in layer 2 necessary for 2D condensation in layer 3 will therefore be substantially larger than $\theta_{1,cr}$, and therefore will never be reached. This means that the islands in higher layers will continue to spread by this mechanism until they reach the edges of the first-

layer islands upon which they sit. The larger down-step barrier $E_{-1,a}$ (42 kJ/mol) then comes into play, which restricts further spreading and allows 2D condensation in layer 3. We mimicked this in our simulations by having atoms which land in layer $i+1$ descend to layer i with unit probability until θ_i exceeds 95% of θ_{i-1}. The value of 95% recognizes that each island must necessarily be slightly smaller than the layer on which it sits if the atoms sit in hollow sites. It implies that the average island is about 40 atoms across. The simulations were not sensitive to this value, provided it is close to unity, since changes in it could be easily compensated for by small changes in the parameter $p_{\rm up}$ (see below).

Another interesting phenomenon occurs at the same time when islands in the second layer appear. This can be seen by comparing the energetics for a Cu atom which lands on the clean ZnO patch to the left in Fig. 9 with that for a Cu atom which lands on the clean ZnO patch to the right. Moving from left to right (to mimic the situation before layer-2 islands form), this Cu atom is first trapped at the island edge, and then experiences a large barrier $E_1=61$ kJ/mol which prevents it from moving up onto the Cu island. This process is therefore precluded at 130 K, but can occur at 300 K and above. On the other hand, let us follow the same process for the Cu atom which lands at the right in the picture and moves left (to mimic the situation after islands form in layer 2). Again, it is trapped at the island edge, but now its up-step barrier E_{1a} is reduced to only about 26 kJ/mol. This is because there is an island edge in the second layer near this step which greatly stabilizes this diffusing Cu atom as it moves into that layer. It is important to realize that this 26-kJ/mol barrier is readily accessible even at 130 K. Thus up-stepping onto islands will be greatly facilitated as soon as islands exist in reasonable concentrations in the layer above.

During vapor deposition, such islands will spontaneously arise due to newly deposited Cu atoms even below 130 K, once θ_1 exceeds 0.55 (see above). However, such islands cannot appear in the annealing experiment of single-layer Cu (Fig. 2) until above 300 K, when the unassisted up-step barrier (E_1) of 61 kJ/mol becomes accessible. The same type of effect occurs in moving from the second layer into the third layer, and beyond, only now the unassisted barrier (E_2) is 66 kJ/mol, and the assisted barrier (E_{2a}) is 31 kJ/mol. Both these values are only slightly larger than in layer 1. To mimic this effect in an approximate way in our simulations, we have made these up-steps impossible at 130 K, unless there is some minimum coverage ($\theta_{\rm min}$) in the layer above. Above this value, every new Cu atom which goes into the layer below is assumed to make this up-step into this layer above with some high probability $p_{\rm up}$. Of course, the situation is more complex because (1) previously deposited Cu atoms can now move into "upper" layers, and (2) the 3D clusters will not always have top-layer Cu islands properly located near their perimeters to allow such up-steps. We are assuming for simplicity that these two effects are properly balanced in the single parameter $p_{\rm up}$ Its value was adjusted to 0.9 in order to properly fit the slope of the oxygen ISS signal after the break point in Fig. 1. We used $\theta_{\rm min}=0.01$ in our modeling, but the results were very insensitive to its value, provided it was small. Since the average island size assumed above prevents stacking layer i with more than 95% of the coverage of layer $i-1$, atoms which come into any layer i which already has 95% of the coverage of layer $i-1$ are forced to move up into layer $i+1$ with unit probability, so long as layer $i+1$ already has a coverage exceeding $\theta_{\rm min}$; otherwise, it moves down to layer 1.

An interesting feature of the growth mechanism we propose here is seen in Fig. 8, where the concentration in each layer grows up to ~55% of a monolayer, and nearly stops as the next layer fills to about the same coverage, and so on. This leads to thick, flat islands that only cover part of the surface. Recent STM observations of metal films deposited on metal substrates that were predosed with ordered oxygen overlayers indeed show such behavior,[43] and may be explained by our new model.

This type of flat island structure has important consequences for understanding the annealing behavior (Figs. 2 and 3). Starting from this structure, the only way the average thickness of the clusters can get much larger upon heating is for Cu atoms from the top-layer islands to be thermally activated up onto that layer as 2D lattice-gas adatoms, where they can diffusively encounter each other and eventually nucleate an island on that new layer. As soon as this occurs, this island will be populated rapidly from the layers below until it reaches the edges of the island below. Then further up-growth must await the nucleation of a new layer's island. These nucleation steps must be slow, and in any case they cannot occur until the unassisted up-step barrier is accessible. This barrier is 61 kJ/mol for layer 1, and 66 kJ/mol in subsequent layers, so they should become available on the seconds time scale of the annealing experiments at about 300 K, which is consistent with the observed onset of clustering in Figs. 2 and 3 at about this temperature.

It is perhaps confusing that these islands do not reach their full thickness within the next 100 K, since all the barriers involved should then be so easily scaled. Instead, after the initial rapid increase at ~300 K, the islands gradually get thicker and thicker up to ~800 K (Figs. 2 and 3). The amount by which they thicken is rather small in any 100-K increment, suggesting a low activation energy for the rate-limiting step. This would be contradictory to the fact that the process is not complete until above 800 K. However, this confusing result is not unique to the Cu/ZnO system. For example, Diebold, Pan, and Madey[17] observed a very similar annealing behavior between 370 and 570 K for Cu on TiO_2(110), and estimated an apparent activation energy of only 13 kJ/mol for clustering. Similarly, Shamir *et al.*[44] showed that four monolayers of Cu deposited onto a nitrided W(110) surface clustered into much thicker islands gradually between 350 and 700 K. Similar behavior was seen for Cu on Re(0001) by He and Goodman.[45]

These unusual kinetics above 350 K thus seem to be a property of Cu films, and unrelated to the choice of substrate. It may be quite a difficult behavior to clarify due to the necessity for top-layer nucleation. Spontaneous

nucleation is well known to be a complex kinetic phenomenon.[48,49] The dramatic increase at ~300 K may be due to Cu from layer 1 moving up to complete the second layer of those clusters which already had nucleated a small second-layer island at the end of the deposition. Thereafter, further clustering is rate limited by the nucleation of clusters in layer 3, which is inherently much slower. A related kinetic model has been developed by Ahn and co-workers to explain the coarsening of Pt particles on alumina.[48,49] Their model and experimental data show that the rate of clustering at a fixed temperature decreases dramatically with the extent of clustering. In experiments such as those illustrated in Figs. 2 and 3 and those referred to above, the extent of clustering necessarily increases with temperature. Thus, the weak apparent temperature dependence above 350 K is probably an artifact of the decrease in clustering rate with the extent of clustering, rather than a consequence of a low activation energy for the rate-determining step.

We have attributed the annealing behavior of the work function (Fig. 2, inset) entirely to the uncovering of more and more clean ZnO. The smooth increase in the work function also undoubtedly has contributions at low temperature from island compaction or coarsening, and at high temperature from conversion of the Cu parts of the surface from (110)-like to (111)-like. Note that Cu(111) has a work function which is about 0.5 eV above Cu(110).[8] The TPD behavior of this Cu film after CO adsorption indicates that the number of Cu(110)-like sites for CO decreases, and the number of (111)-like sites grows as the layer is annealed between 460 and 650 K.[6] Room-temperature LEED and ARXPS studies show that the Cu films take on (111) structure only when the islands are four or more layers thick (see above).

A final important feature of Fig. 9 is the barrier size for the assisted Cu→ZnO down-step, E_{-1a}, of ~42 kJ/mol. It is this down-step which is required for CO to redisperse second-layer Cu into the first layer. This barrier is perhaps slightly too large to occur frequently enough without CO assistance at the temperature of CO dosing (130 K, Ref. 6). Weakly adsorbed states of CO existing at high CO coverage should help decrease this barrier further via the energy gained in CO adsorption when new Cu sites are thus created. Only 20% of the 50-kJ/mol heat of CO adsorption would be needed for stabilization at the transition state to reduce this barrier to 32 kJ/mol, which is easily accessible at 130 K.

D. Application of this model to other systems

The growth of Pd on ZnO(000$\bar{1}$) has been studied at 300 K and above by Jacobs *et al.* using AES and LEED.[29] It was concluded after deposition of the equivalent of one monolayer (ML) of Pd at 300 K that 3D islands with an average thickness of 5 ML were formed which left ~80% of the surface free of Pd. Only after 35 equivalent monolayers of Pd did new LEED spots for the overlayer appear, and these were indicative of thick Pd(111)-terminated islands rotationally aligned with the ZnO lattice. This strong tendency for Pd to make 3D clusters on ZnO(000$\bar{1}$) is rather surprising in light of the fact that Cu (see above) and Pt (Ref. 50) both grow in a 2D film at this same temperature (300 K) on this surface, until ~45% and 100%, respectively, of the surface is covered. In both those systems, electron-diffraction patterns indicating (111)-oriented metal islands were seen after only a few monolayers of deposition,[50] not 35 monolayers as with Pd.[29] These dramatic differences between these three similar metals (Pd and Cu or Pt) have not been explained and bear further discussion in light of our model for Cu. The differences could simply be due to the fact that the energy difference ΔE (see Fig. 9) between the metal-metal and metal-ZnO interactions is smaller than the 2D condensation energy E_i in the case of Cu and Pt, but larger in the case of Pd. It is this negative energy difference which drives 2D spreading at low coverages for Cu and Pt within our model. It is therefore not necessary to postulate a qualitative difference in the thermodynamic tendency between these similar metals on ZnO, since thermodynamics seems to be in favor of 3D clustering in all three cases at high temperature.[29,50] Now ΔE should scale roughly with the heat of oxide formation, which goes as Pt > Pd > Cu, whereas E_i should scale with the sublimation energy, which goes as Pt > Pd > Cu. Thus E_i may exceed ΔE for Cu because ΔE is small, whereas it occurs for Pt because E_i is large. In the intermediate case of Pd, it may not occur.

The very confusing state of knowledge concerning metal deposition on oxides has recently been reviewed,[1] where it was pointed out that the systems which show Stranski-Krastonov (or laminar) or Volmer-Weber growth (3D clustering) at 300 K cannot yet be predicted in any way. Based on our new model, it is important to recognize that the wetting observed in many of those cases may only be a dynamical result, and not any indication that the metal-oxide adsorption bond is stronger than the metal-metal bond. According to our model, spreading will be expected over a large fraction of the first monolayer at low temperatures, where the unassisted up-steps (E_1 and E_2) are prohibited, whenever E_i exceeds ΔE, not just when ΔE is negative. Since E_i is quite large for metals like Pt (~160 kJ/mol, based on embedded-atom calculations[36]), the requirements on ΔE for apparent wetting are consequently much less stringent. In the model we present above, the down-step barrier E_{-1} must also be accessible at the temperature of deposition. However, even this requirement is removed by recent trajectory calculations for Pt growth on Pt(111), which show that the adsorption energy of the incoming Pt atom can easily be used to push aside atoms in islands in the layer below where it hits. This allows the new Pt atom to move into that layer below with high probability even at zero substrate temperature.[36] Since Pt should diffuse more readily on an oxide surface to which it is more weakly bonded, this dynamical effect may be even more important on oxides, since the energy for pushing atoms aside should be reduced. Another dynamical effect referred to as "downward funneling" can also assist incident atoms to spread to the layer below.[51]

These dynamical effects very much relax the con-

straints in our model on the magnitudes of the barriers E_{-1} and E_{-2}, and the barrier for diffusion of Cu over Cu. That is, if these dynamical effects were included, the uptake data of Fig. 1 could be modeled even if these barriers exceeded 32 kJ/mol. This would, of course, lead to much rougher high-coverage films than those with the flat tops that we predicted above, assuming that these barriers were small. Microscopic measurements of the film structure should be able to reveal which of these two situations is really obtained. In any case, in modeling the uptake data it is necessary that Cu be able to easily diffuse across ZnO(0001)-O at 130 K, or at least that incident Cu atoms have enough transient mobility to find the edge of islands before stopping in the first layer. It is also necessary that these Cu atoms be able to make assisted up-steps (E_{1a} and E_{2a}), either via transient mobility or because these barriers are accessible at the growth temperature. It is also critical for our model that E_i exceed ΔE in magnitude, and that the unassisted up-steps (E_1 and E_2) be kinetically prevented at the growth temperature. Other systems which meet these constraints should show similar growth behavior. These classes of systems need not be limited to metal films on oxide substrates.

V. CONCLUSIONS

Thermodynamic considerations indicate that Cu does not wet ZnO(0001)-O at equilibrium. However, when it is vapor deposited onto this surface at 130 K, it first covers most of the surface in 2D metallic islands. When these cover about 55% of the surface, the islands abruptly start to thicken, and the Cu which lands on clean ZnO patches between these islands migrates onto these islands with high probability ($\sim$90%). This results in thick, flat islands covering most of the surface, with clean ZnO between. These islands thicken, take on more (111)-like character, and cover less of the surface after annealing thin or thick layers to above room temperature. These and other results are well explained using a simple kinetic model based on the known energy barriers of Cu on pure Cu for diffusion, 2D evaporation from kinks onto terraces, and migration over island edges. It is assumed that Cu on this ZnO surface is about 16 kJ/mol less stable than Cu on Cu, and that similar migration steps at the Cu/ZnO interface have energy barriers that differ from those on pure Cu by two thirds of their difference in reaction energies. The model shows that for systems such as metals on oxides that tend not to wet effectively: (1) efficient wetting can still occur in the first layer at low temperatures whenever the 2D evaporation energy for the metal exceeds the stability difference between the metal on itself and on the oxide; (2) this spreading will cease at a certain critical 2D island size even when the diffusion barrier on terraces is negligible, and further growth will cause the creation of thick, flat islands, filling in the gaps between these islands only very slowly.

ACKNOWLEDGMENTS

The authors would like to thank Professor Hannes Jonsson and Professor Thomas Engel for many useful insights concerning metal growth and diffusion dynamics and energetics. We also thank Dr. Scott Chambers and Professor Marjorie Olmsted for insightful discussions concerning x-ray-photoelectron diffraction. Financial support for this research by the Department of Energy, Office of Basic Energy Sciences, Division of Chemical Sciences is gratefully acknowledged. K.H.E. thanks the German Research Foundation (DFG) for financial support.

[1]C. H. F. Peden, K. B. Kidd, and N. D. Shinn, J. Vac. Sci. Technol. A **9**, 1518 (1991).

[2]C. T. Campbell, K. A. Daube, and J. M. White. Surf. Sci. **182**, 458 (1987).

[3]S. V. Didziulis, K. D. Butcher, S. L. Cohen, and E. I. Solomon, J. Am. Chem. Soc. **111**, 7110 (1989).

[4]This can be readily proven following the development of C. Herring and M. H. Nichols, Rev. Mod. Phys. **21**, 185 (1949), Secs. I.2, II.4-5,11.

[5]W. Hirschwald, in *Current Topics in Materials Science,* edited by E. Kaldis (North-Holland, Amsterdam, 1981), Vol. 7, Chap. 3.

[6]A. Ludviksson, K. H. Ernst, R. Zhang, and C. T. Campbell, J. Catal. **141** (1993).

[7]R. Zhang, A. Ludviksson, and C. T. Campbell, Surf. Sci. (to be published).

[8]H. B. Michaelson, J. Appl. Phys. **48**, 4731 (1977).

[9]H. Mooremann, D. Kohl, and G. Heiland, Surf. Sci. **80**, 261 (1979).

[10]P. A. Thiel and T. E. Madey, Surface Sci. Rep. **7**, 211 (1987).

[11]W. Hirsch, Ph.D. thesis, Freien University, Berlin, 1987.

[12]J. M. Vohs and M. A. Barteau, Surf. Sci. **176**, 91 (1986).

[13]J. A. Rodriguez, W. D. Clendening, and C. T. Campbell, J. Phys. Chem. **93**, 5238 (1989).

[14]M. T. Paffett and C. T. Campbell, J. Vac. Sci. Technol. A **3**, 812 (1985).

[15]H. H. Brongersma and P. M. Mul, Chem. Phys. Lett. **14**, 380 (1972); D. G. Schwartzfager, Anal. Chem. **56**, 55 (1984).

[16]U. Bardi, Appl. Surf. Sci. **51**, 89 (1991).

[17]U. Diebold, J.-M. Pan, and T. E. Madey, Phys. Rev. B **47**, 3868 (1993).

[18]W. Mokwa, D. Kohl, and G. Heiland, Fresenius Z. Anal. Chem. **314**, 315 (1983).

[19](a) C. D. Wagner, R. M. Riggs, L. E. Davis, J. F. Moulder, and G. E. Muilenberg, *Handbook of X-Ray Photoelectron Spectroscopy* (Perkin-Elmer, Eden Prairie, MN, 1979) (see the references that accompany the table of Cu Auger parameter data on p. 171 of this book); (b) C. D. Wagner, Faraday Disc. Chem. Soc. **60**, 291 (1975); (c) B. R. Strohmeier, D. Leyden, R. S. Field, and D. M. Hercules, J. Catal. **94**, 514 (1985).

[20]G. Moretti, Surf. Interf. Anal. **17**, 352 (1991); G. Moretti, A. Y. Stakheev, and W. M. H. Sachtler, J. Electron. Spectrosc. Relat. Phenom. **58**, R1 (1992).

[21]P. Zurcher and R. S. Bauer, J. Vac. Sci. Technol. A **1**, 695 (1983).

[22]Since the Fermi level is largely determined from the position of the oxygen vacancies in these vacuum annealed samples to be just below the bulk conduction-band minimum, and since

the vacuum level tracks the band energies near the surface (Ref. 23), the slightly larger work function of our sample compared to vacuum-cleaved samples implies that our bands are bent upwards slightly more than the −0.22-eV value reported (Ref. 9) for the cleaved sample.

[23]J. Scheer and J. Van Laar, Surf. Sci. **18**, 130 (1969).

[24]W. Moench, Rep. Prog. Phys. **53**, 221 (1990).

[25]H. Onishi, T. Aruga, C. Egawa, and Y. Iwasawa, Surf. Sci. **233**, 261 (1990).

[26]S. A. Chambers, Adv. Phys. **40**, 357 (1991); W. F. Egelhoff, Crit. Rev. Solid State Mater. Sci. **16**, 213 (1990).

[27]J. A. Rodriguez and C. T. Campbell, J. Phys. Chem. **91**, 6648 (1987).

[28]C. T. Campbell, Ann. Rev. Phys. Chem. **41**, 775 (1990).

[29]H. Jacobs, W. Mokwa, D. Kohl, and G. Heiland, Surf. Sci. **160**, 217 (1985); (see also Ref. 46).

[30]A. Gutmann, G. Zwicker, D. Schmeisser, and K. Jacobi, Surf. Sci. **137**, 211 (1984).

[31]J.-P. Coulomb, T. S. Sullivan, and O. E. Vilches, Phys. Rev. B **30**, 4753 (1984).

[32]A. Ludviksson, R. Zhang, and C. T. Campbell (unpublished).

[33]M. P. Seah and W. A. Dench, Surf. Interf. Anal. **1**, 2 (1979).

[34]J. M. Campbell, J. Nakamura, and C. T. Campbell, J. Catal. **136**, 24 (1992).

[35]B. Poelsma, R. Kunkel, N. Nagel, A. F. Becker, G. Rosenfeld, L. K. Verheij, and G. Comsa, Appl. Phys. A **53**, 369 (1991).

[36]M. Villarba and H. Jonsson (private communication).

[37]The self-diffusion barrier on Cu(100) is 30 kJ/mol (Ref. 39), and the diffusion barrier on Cu(111) is less than 30% of that on Cu(100) (Ref. 38).

[38]D. W. Bassett and P. R. Weber, Surf. Sci. **70**, 520 (1978).

[39]H.-J. Ernst, F. Fabre, and J. Lapujoulade, Phys. Rev. Lett. **69**, 458 (1992).

[40]This can be estimated on small islands to be the energy on pure Cu for evaporation of kink atoms from domains onto terraces (0.55 eV (Ref. 39)).

[41]This assumes that the ratio of these two barriers is the same on Cu and Pt. This ratio was calculated to be about 1:4 on Pt(111) using the embedded-atom method (Ref. 36).

[42]W. C. Gardiner, *Rates and Mechanisms of Chemical Reactions* (Benjamin, Menlo Park, CA, 1972).

[43]R. Q. Hwang, C. Gunther, J. Schroeder, E. Kopatzi, and R. J. Behm, J. Vac. Sci. Technol. A **10**, 1970 (1992).

[44]N. Shamir, J. C. Lin, and R. Gomer, Surf. Sci. **214**, 74 (1989).

[45]J. W. He and D. W. Goodman, J. Phys. Chem. **94**, 1496 (1990).

[46]An earlier paper by Gaebler, Jacobi, and Ranke (Ref. 47) about Pd/ZnO(0001)-O strongly contradicts the results of Jacobs *et al.* (Ref. 29) in that their AES uptake curve is interpreted in terms of layer-by-layer growth.

[47]W. Gaebler, K. Jacobi, and W. Ranke, Surf. Sci. **75**, 355 (1978).

[48]T.-M. Ahn, S. Purushothaman, and J. K. Tien, J. Phys. Chem. Solids **37**, 777 (1976).

[49]T.-M. Ahn, P. Wynblatt, and J. K. Tien, Acta Metall. **29**, 921 (1981).

[50]S. Roberts and R. J. Gorte, J. Chem. Phys. **93**, 5337 (1990).

[51]D. E. Sanders and J. W. Evans, Surf. Sci. **24**, 38 (1991).